Author/s:
Islam, A;Pattnaik, N;Moula, MM;Rötzer, T;Pauleit, S;Rahman, MA

Title:
Impact of urban green spaces on air quality: A study of PM10 reduction across diverse climates

Date:
2024-12-10

Citation:
Islam, A., Pattnaik, N., Moula, M. M., Rötzer, T., Pauleit, S. & Rahman, M. A. (2024). Impact of urban green spaces on air quality: A study of PM10 reduction across diverse climates. Science of the Total Environment, 955, pp.1-13. https://doi.org/10.1016/j.scitotenv.2024.176770.

Persistent Link:
https://hdl.handle.net/11343/354155

Science of the Total Environment 955 (2024) 176770

Contents lists available at ScienceDirect

Science of the Total Environment

journal homepage: www.elsevier.com/locate/scitotenv

Impact of urban green spaces on air quality: A study of PM10 reduction across diverse climates

Azharul Islam [a,*], Nayanesh Pattnaik [a], Md. Moktader Moula [b], Thomas Rötzer [c], Stephan Pauleit [a], Mohammad A. Rahman [a,d]

[a] Strategic Landscape Planning and Management, School of Life Sciences, Weihenstephan, Technische Universität München, Emil-Ramann-Str. 6, 85354 Freising, Germany
[b] Institute of Forestry and Environmental Sciences, University of Chittagong, Chittagong, Bangladesh
[c] Forest Growth and Yield Science, School of Life Sciences, Weihenstephan, Technische Universität München, Hans-Carl-von-Carlowitz-Platz 2, 85354 Freising, Germany
[d] The University of Melbourne, Burnley, Victoria, Australia

HIGHLIGHTS

- PM_{10} concentration and deposition flux were highest in Hong Kong and lowest in Vancouver.
- PM_{10} flux showed a positive relationship with population density, LST & wind pressure.
- Park site showed the lowest PM_{10}, while industrial site showed the highest.
- Greenspace contribution was significant once the greenspace cover exceeded 27 % of the land cover.

GRAPHICAL ABSTRACT

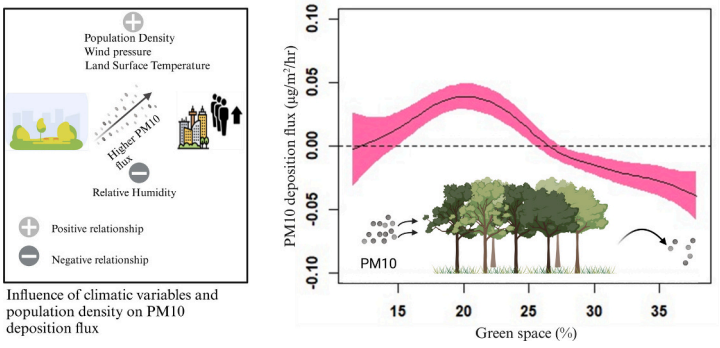

Influence of climatic variables and population density on PM10 deposition flux

ARTICLE INFO

Editor: Alessandra De Marco

Keywords:
Urban air quality
PM10
Population density
Urban greenspaces
Climatic variables
GAM

ABSTRACT

Urban areas face high particulate matter (PM10) levels, increasing the risk of respiratory and cardiovascular diseases. Green spaces can significantly reduce PM10 concentration, as shown at various scales, from boroughs to whole cities. However, long-term monitoring is needed to understand the specific mechanisms and cumulative impact of green spaces on air quality to changing pollution levels. We investigated the influence of neighbourhood green space percentage, climatic variables, and population density on PM10 deposition during the vegetation period across eight cities in contrasting climate zones over 20 years (2000-2020). We used a correlation matrix, generalized additive model, one-way ANOVA, and Tukey HSD test to analyze the impact of these factors on PM10 deposition rates, assess the role of green space percentage in reducing it, and identify significant differences in PM10 parameters at different proximities to emission sources. Cities with higher population density in warmer, drier climates had higher PM levels, since land surface temperature and wind pressure positively correlated with PM10 deposition, while relative humidity showed a negative correlation. The study found significantly higher PM10 concentrations in industrial areas (36.25 µg/m^3) than in roadside areas (25.73

* Corresponding author.
E-mail addresses: azharul.islam@tum.de (A. Islam), nayanesh.pattnaik@tum.de (N. Pattnaik), thomas.roetzer@tum.de (T. Rötzer), pauleit@tum.de (S. Pauleit), ma.rahman@tum.de (M.A. Rahman).

https://doi.org/10.1016/j.scitotenv.2024.176770
Received 10 July 2024; Received in revised form 10 September 2024; Accepted 4 October 2024
Available online 10 October 2024

μg/m^3) and parks (20.17 μg/m^3) ($p < 0.01$). This highlights the need for targeted interventions in different zones. The study found a complex relationship between green space percentage and PM10 deposition rate onto plant surfaces. Our model suggests that at least 27% of green spaces as land cover can significantly reduce the particulate matter flux, although the minimum threshold can vary depending on the specific urban contexts. The study focused on the proportionate cover of green spaces; still, further investigation including quantitative aspects of urban surface forms, and traffic emissions can comprehend the climatic context and determine the optimal extent of green space required for strategic planning toward future urban sustainability initiatives.

1. Introduction

The trend of the world's population living in urban areas is ever-increasing, projected to reach 66 % by 2050 (United Nations, 2018). Higher population density due to urbanization leads to higher particulate matter (PM) concentrations (Baek and Ban, 2020). In particular, PM10, a particular type of airborne pollutant comprising small particles with an aerodynamic diameter of 10 μm or less (Anderson et al., 2012), is regarded as a contributor to respiratory and cardiovascular diseases (Chowdhury et al., 2018; Cowell et al., 2019). Moreover, green space is often limited in densely populated urban areas (Arshad and Kumar Routray, 2018). Green spaces help mitigate PM10 by increasing deposition surfaces (Janhäll, 2015) and enhancing urban surface roughness (Gunawardena et al., 2017). In Rome, Marando et al. (2016) reported 3757.4 Mg PM10 removal by 22 % of vegetation cover during summer. McDonald et al. (2007) showed that increasing tree cover in Glasgow from 3.6 % to 8 % could reduce 2 % average annual PM10 concentration. Thus, urban vegetation appears to be one of the promising action-based techniques since preventive and mitigating strategies for PM emissions pose substantial challenges (Wu and Guo, 2021).

PM deposition flux (the rate at which PM is removed from the atmosphere and deposited onto a surface area over a specific time) can be influenced by temporal variations of PM, along with meteorological conditions, green space proximity, and deposition surface availability (Erisman and Draaijers, 2003; Zellner, 1986). Local meteorological conditions, such as land surface temperature (uplift), precipitation (washout), and wind pressure (dispersing), influence the level of PM (Faisal et al., 2022; Li et al., 2019; Zhang et al., 2015). A study by Wang et al. (2015) demonstrated that intense rainfall events can wash out accumulated coarse particles by 28–48 % from a single species, while higher wind pressure can remove them by 27–35 %. Xu et al. (2017) showed that wash-off by controlled rainfall removed 51 to 70 % of surface PM accumulation from the foliage of four broadleaf species. Chithra and Shiva Nagendra (2014) found a positive association between indoor PM10 and outdoor temperature, with an R^2 value ranging from 0.32 to 0.47. At the same time, urban vegetation can significantly improve the local climate, for instance, providing shade and cooling effects through increasing evapotranspiration (Pace et al., 2021; Rahman et al., 2023) which might reduce the formation of secondary PM.

The presence of green space or individual plant elements interacting with PM as a system can facilitate temporary or permanent deposition of PM10 onto a plant surface, and the leeward side of green space affects dispersion, which can reduce PM10 concentration (Diener and Mudu, 2021; Rafael et al., 2018). Leaf particulate matter accumulation increases from spring to autumn during the vegetation period (Wang et al., 2013). Using a monthly PM10 concentrations dataset containing 1216 air quality stations across Europe in 2018, Sohrab et al. (2023) showed that land use significantly impacts air quality, specifically PM10 concentrations. However, the intricate relationships between meteorological parameters, landscape metrics with the land use and land cover composition are largely unknown.

While the general consensus supports the notion that green spaces contribute to improving air quality by reducing PM10 levels (Diener and Mudu, 2021), there are notable inconsistencies (such as reducing ventilation, thus leading to a higher concentration of PM at pedestrian levels (Gromke and Ruck, 2009) and knowledge gaps in the scientific literature (Wang et al., 2024). For instance, in terms of spatial scale, studies conducted at different spatial scales (local, urban, regional) often yield varying results. Some studies report significant PM10 reductions within the immediate green spaces, while others find limited or no impact at larger scales. This discrepancy may be attributed to factors such as the type of green space (e.g., sparse vegetation versus large urban forests), meteorological conditions (Nguyen and Liou, 2024), and the distribution of pollution sources. Green spaces appear to be more effective in mitigating traffic-related PM10 emissions, with experimental evidence indicating up to a 50 % reduction in time-averaged PM concentrations near roadside vegetation (Deshmukh et al., 2019; Ottosen and Kumar, 2020). However, their effectiveness is less pronounced for industrial emissions, which may even show a negative correlation with PM10 levels, particularly during summer when heating is not required (Sohrab et al., 2023). Uncertainty also exists regarding the complex interplay between vegetation with inherent traits such as leaf area index, tree spacing and different PM10 sources while minimizing the negative impact on air quality (Vashist et al., 2024; Wang et al., 2024; Zhao et al., 2024). Moreover, most studies focus on the short-term effects of green spaces on PM10 (Vitaliano et al., 2024). There is a need for long-term monitoring to assess specific mechanisms as well as their relative and cumulative importance of green spaces on air quality to changing pollution levels. Local studies are important to understand the deposition effects; however, studies encompassing various species in various setups and climatic zones along with population density, which can serve as a surrogate measure for other emission sources in the urban environment are vital for comprehensive long-term policy-making (Vashist et al., 2024).

A study by Pražnikar (2017) demonstrated the inter-continental comparison of PM in semi-arid and humid-continental climate zones. Another study by Wang et al. (2021) showed how PM10 differs across cities located in eight climatic regions of China. Therefore, a relatively long-term study to understand the impact of urban green spaces on PM10 removal across diverse climates is absolutely necessary. Additionally, Sohrab et al. (2022) found that road density and proximity strongly affect PM10 levels, with pollution decreasing as distance from roads increases in urban and rural areas. In densely populated residential zones, higher traffic volumes and congestion elevate PM10 levels. However, there is a knowledge gap regarding the spatial placement of vegetation within different climate zones to improve air quality without disrupting the daily lives of residents.

We hypothesized that with increasing temperature and wind pressure (hence lower wind speed) but decreasing relative humidity, PM10 deposition flux will increase, green spaces closer to the sources will also increase the deposition, and finally, more dense green spaces will have better PM10 reduction compared to sparse canopies. The hypothesis will be tested using 20 years of long-term data on green spaces and PM10 concentrations, analyzed at both citywide and local scales across eight cities located on different continents, each with distinct setups and climate zones. This study aims to investigate: 1. How green space density, climatic variables, and population density influence PM10 deposition flux during the vegetation period and 2. What are the optimal locations for tree planting—parks, roadsides, or industrial sites—to achieve the most effective reduction in PM10 levels?

2. Materials and methods

2.1. Study area and sampling sites selection

Larger and densely built cities typically have higher levels of PM10 concentration since PM10 flux tends to increase with higher emissions from transportation, energy consumption and intensified land use per area unit (An et al., 2013). As such, we collected PM10 concentration data from eight cities (≥2 million population in 2020) located within contrasting Köppen-Geiger major climate zones (Fig. 1) (Peel et al., 2007). These global metropolises offer diverse urban settings, planning approaches, and robust data, enabling broad applicability of study findings.

The available PM10 data was utilized to select sample sites. Specifically, cities located in different climate zones that had publicly available PM10 concentration data up to at least the last 20 years (2000 to 2020) were selected. Three stations in each city: Berlin, London, Stockholm, Melbourne, Vancouver, New York City, Hong Kong, and Los Angeles (See Supplementary Tables 1 and 2 for details) were selected. A one-kilometre buffer area was created around each air quality monitoring station, with the station coordinates serving as the centre of each buffer area (Fig. 2).

Studies showed the influence of land use and greenspaces on PM concentration was more suitable for buffers starting from 1000 m (Connors et al., 2013; Lei et al., 2018; Sohrab et al., 2023). The one-kilometre buffer was chosen because this study wanted to concentrate the analysis on a neighbourhood scale rather than a city scale (2000–16,000 m), which the 1000 m buffer accurately captures.

To address research question two, London was focused on due to data availability along different emission sources, and three distinct sampling sites (park, roadside, and industrial) were selected (Supplementary Fig. 1) (London Air Quality Network, 2023). We created a 150 m buffer area around the position of the air quality monitoring stations. Here, the focus was to conduct a detailed investigation of how PM10 concentrations, PM10 deposition flux, and PM10 dry deposition vary at different proximity levels from emission sources in a city located within a particular climate zone. In London, we selected a 150 m buffer to utilize fine-scale resolution data for determining PM10 dry deposition, accounting accurate leaf area index (LAI). However, park, roadside, and industrial sites were selected since this approach can provide insights into the very localized effect of green space compared to other land uses.

2.2. PM10 data

PM10 concentration data for selected cities was obtained from open sources (Supplementary Table 2). Since plants experience strong growth during the growing period and reach their peak dust absorption capacity in the summer (Gao et al., 2015), the study focused on the vegetation period.

For the vegetation period, we selected five months (even though the vegetation period usually decreases from South to North) (Rötzer and Frank-M. Chmielewski., 2001) from April to August to represent the vegetation period for Berlin, London, New York, Los Angeles, and Vancouver. For Stockholm and Hong Kong, the representative vegetation period was selected from May to September. Lastly, the vegetation period from October to February was selected for Melbourne. Initially, we calculated the monthly mean PM10 concentration. Afterwards, the mean PM10 concentration during the vegetation period was determined. Vegetation period was also selected to account for the differences in leaf-bearing duration between evergreen conifers and deciduous trees.

Among the selected stations, only Stockholm and New York had subsequent missing data in their monthly mean PM10 concentration. For Stockholm, the PM10 data availability was from 2006 to 2020. Therefore, the imputation method for the missing monthly mean PM10 for Stockholm was utilized (following Kang, 2013). Additionally, missing PM10 concentration data for New York was substituted with the sum of emitted PM10 from all anthropogenic sources documented by EDGARv6 (https://eccad.sedoo.fr/#/catalogue).

2.3. Population density data

Population density data within each one-kilometre buffer area was extracted using Google Earth Engine from "GPWv411: UN-Adjusted Population Density".

(Gridded Population of the World Version 4.11) database (CIESIN/GPWv411/GPW_UNWPP-Adjusted_Population_Density). This dataset provided population density values at a spatial resolution of approximately 1 km (927.67 m) and a unit of persons per square kilometre. The population density within each one-kilometre buffer zone was calculated by averaging the population density values across all grid cells using the ee.Reducer.mean () function in Google Earth Engine. The population data was estimated based on national censuses for 2000, 2005, 2010, 2015, and 2020. Subsequently, linear imputation was

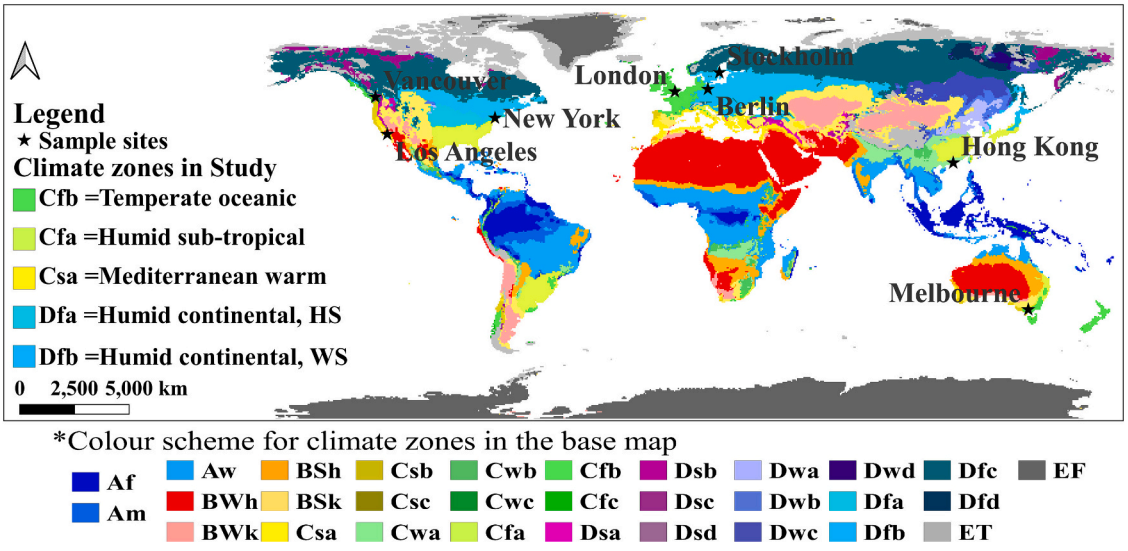

Fig. 1. Location of the studied sample sites.
*Indicated that the colour scheme was adopted from Peel et al., 2007. A colour represents a climate zone.

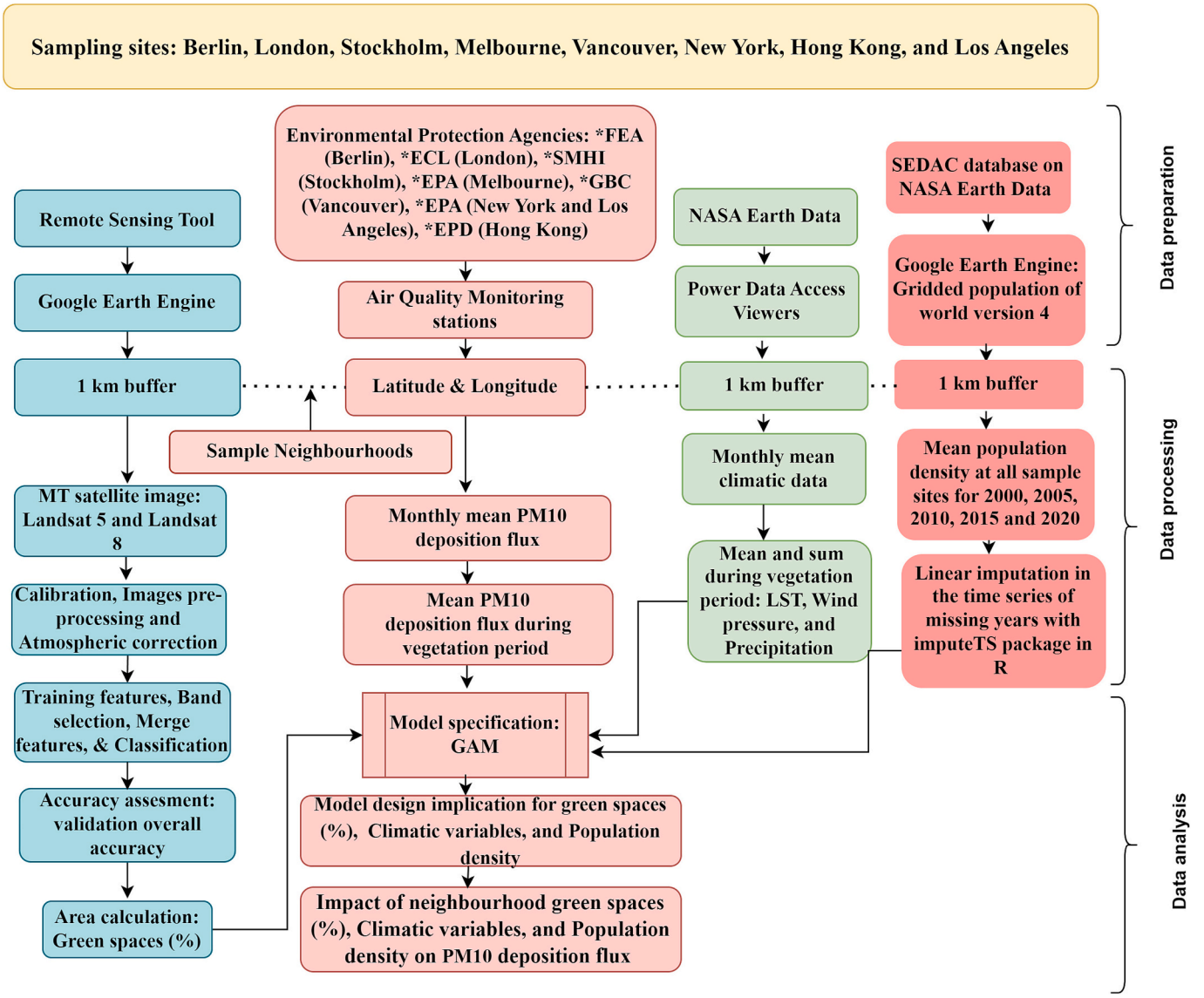

Fig. 2. The methodological framework for extracting greenspace percentage using Google Earth Engine and analyzing the impact of neighbourhood green space (%), climatic variables, and population density on PM10 deposition flux using the GAM model.
Here, *FEA, *ELC, *SMHI, *EPA, *GBC, *EPA, and *EPD indicated Federal Environmental Agency, Empirical College of London, Swedish Meteorological and Hydrological Institute, Environmental Protection Authority, Victoria, Government of British Colombia, Canada, Environmental Protection Agency, USA and Environmental Protection Department, Hong Kong respectively.

performed for missing values in the time series of population data using the imputeTS package in R (Moritz and Bartz-Beielstein, 2017).

2.4. Climatic variables data

This study also assessed meteorological variables: land surface temperature (°C), precipitation (mm/day), and wind pressure (kPa) as the climatic variables of interest during the vegetation period (Supplementary Tables 5 and 11). The climatic variables data was obtained from the Data Access Viewer of NASA Prediction of Worldwide Energy Resources-the Power project. (https://power.larc.nasa.gov/data-access-viewer/). Here, the coordinate points of each sample site represented the specific target points from which climatic variables data were collected, including mean land surface temperature (LST), mean wind pressure during the vegetation period, and mean precipitation in mm/day. Consequently, precipitation data was aggregated as a sum over the vegetation period. Wind pressure, instead of wind speed, was used as pressure is often related to low wind speed and significantly affects the atmospheric stability conditions which influence the pollutant concentration (Akyüz and Çabuk, 2009).

2.5. Land use and land cover analysis

To obtain green space data, pixel-based land use and land cover (LULC) classification analysis was conducted using Landsat 5 and Landsat 8 from 2000 to 2020 in Google Earth Engine. Subsequently, we focused on four major land cover types, namely green space, built-up area, bare soil, and water (Fig. 3). The cloud cover of the satellite images was ensured to be <10 %; however, only in exceptional cases, up to 17 % cloud cover was considered. The visual proportions of land cover types (based on the proportional representation of each land cover type) were considered at the sample site to assign training points for each class. Afterwards, we used a random forest classifier to conduct classification using the assigned training points. Trees, shrubs, and grass were included within the green space class (Fig. 2 and Supplementary code 4).

The accuracy of the land cover classification was checked once be-

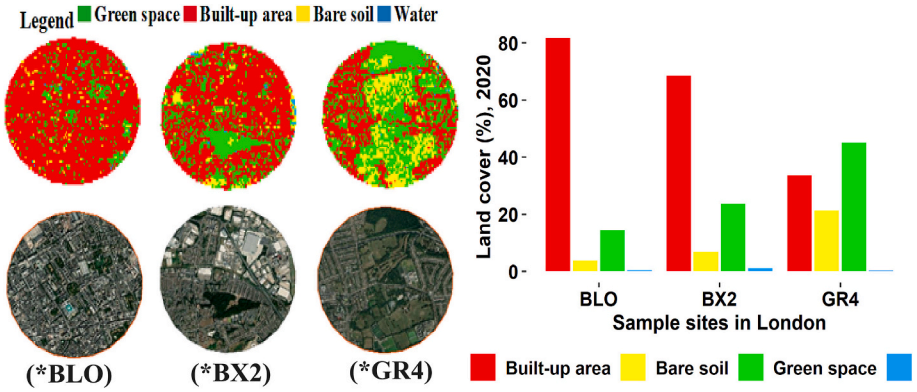

Fig. 3. An example image of extracted greenspaces from sample sites in London through pixel-based LULC. Here, (*BLO), (BX2), and (*GR4) indicate sample sites ID for 1 km buffer in London.

tween 2000 and 2020 with training overall accuracy, training kappa, confusion matrix, validation error matrix, and validation overall accuracy. The validation overall accuracy was 0.973, 0.952, 0.962, 0.921, 0.995, 0.952, 0.948, and 0.939 for the sample sites in Berlin, Hong Kong, London, Los Angeles, Melbourne, New York, Stockholm, and Vancouver respectively (Supplementary Table 4). Total green space was converted into total green space percentage Eq. (1):

$$\text{Green space}\ (\%) = \frac{\text{Green space}}{\text{Total land cover}} * 100 \quad (1)$$

2.6. Calculation of PM10 deposition flux and PM10 dry deposition

The dry particle flux of PM10 (mass per area and time) can be expressed as the product of deposition velocity V_d (length per time) and PM10 concentration c (mass per volume) (Langner et al., 2011). Deposition velocity represents the rate at which particles are deposited from the atmosphere to a surface. The downward pollutant flux of PM10 or PM10 deposition flux was calculated using the following formula (Wu et al., 2018; Zufall and Davidson, 1998):

$$F = V_d C \quad (2)$$

where F is the deposition flux of PM10 in $\mu g/m^2/s$, V_d is the dry deposition velocity of PM10 (m/s), and C is the concentration of PM10 in the air. V_d was evaluated at a median value of 0.0064 m/s from the literature (Lovett, 1994). Even though surface types influence deposition velocity and deposition rates, green space was considered to be the only deposition surface since our study aims to assess the unique impact of green space on air quality. To address research question two specifically for the London case study, we calculated PM10 dry deposition over the vegetation period following McPherson et al. (1994) as:

$$\text{PM10 dry deposition per ground area} = \left(\sum_{i=1}^{5} V_d.C_i T_i.24.3600.LAIi.0.5 \right) \quad (3)$$

Here, T_i is the number of days studied, LAI_i corresponds to the calculated leaf area index within the 150 m buffer area during the vegetation period, and 0.5 is the resuspension rate of particles returning to the atmosphere (Zinke, 1967). The resuspension rate refers to the physical process by which a set of particles lying on a surface are entrained away through the action of a fluid flow per unit of time (Henry et al., 2023). LAI was extracted using a remote sensing technique in Google Earth Engine by analyzing Landsat 5 and Landsat 8 surface reflectance imagery from 2000 to 2020. The leaf area index is the total surface area of leaves per unit of ground area. LAI was calculated based on the Enhanced Vegetation Index (EVI), computed as $EVI = 2.5*((NIR - RED)/(NIR + 6*RED - 7.5*BLUE + 1))$ (Andalibi et al., 2021; Huete et al., 1997) (Supplementary Code 1–3). Furthermore, a validation of the LAI values was performed using linear regression between estimated and observed LAI values (De De Peppo et al., 2021) (Supplementary note 1). T_i was estimated between April to August.

2.7. Statistical analysis

We performed statistical analyses using the statistical software R (R 4.2.3).

2.7.1. Correlation matrix and Generalized Additive Model (GAM)

The Spearman correlation matrix was used to obtain a preliminary understanding of the relationship between PM10 deposition flux, population density, and climatic variables. Additionally, the Generalized Additive Model (GAM) (Wood and Augustin, 2002) was employed to capture the non-linear relationships of climatic variables and green space with PM10 deposition flux.

GAMs are a semi-parametric extension of Generalized Linear Models (GLMs) by. incorporating smooth functions in place of linear and other parametric terms (González-Andrés et al., 2021). The smooth function in GAM offers greater flexibility such as it does not need to assume a specific parametric form. The GAM made the only assumption that functions are additive, and components are smooth, which allows the model highly non-linear and non-monotonic relationships between the response and the set of explanatory variables. GAM does not rely on a pre-determined model structure but can be rather described as data driven (Yee and Mitchell, 1991). GAM can be used to estimate the effect on PM10 deposition flux based on a variety of predictor variables to account for potential confounding factors and capture non-linear relationships by incorporating smoothing functions and penalized regression splines (Zuur et al., 2007).

In our model, the response variable was PM10 deposition flux. The predictor variables included green space percentage, as well as population density, and selected climatic variables.

$$g(\text{PM10 deposition flux} = s(\text{Green space percentage}_i) + s(\text{Land surface temperature}_i) + s(\text{Precipitation}_i) + s(\text{Wind pressure}_i) + s(\text{Population density}_i) + \varepsilon \quad (4)$$

The GAMs were fitted with a non-Gaussian distribution and the smoothing function denoted by "s" was incorporated in the explanatory variables for all sampling sites cumulatively. The function g (.) represents the link function in the model, which establishes the relationship between the expected value of the response variable and the predictor variables. The symbol ε represents the residual error term in the model. This term accounts for unexplained variability in the response variable that is not captured by the smooth functions of the predictor variables. The selection of predictor variables for the model was based on a variance inflation factor (VIF) test with a threshold value below 4 to avoid multi-collinearity among predictor variables (O'brien, Robert M., 2007).

To describe the error distribution and the link function to be used in the model, the "scat" family function was used instead of the default Gaussian or the Gamma family function. This choice enhanced the model's ability to capture the complex relationship between PM10 deposition flux and predictor variables. Since the response variable PM10 deposition flux did not follow either Gaussian or skewed distribution, but rather exhibited heavy-tailed distribution. The best model was selected based on the lowest Akaike Information Criterion (AIC) (Burnham and Anderson, 2004), and the model fit was checked with a quantile of a standard normal distribution (Augustin et al., 2012) using the DAHRa package in R (Hartig and Hartig, 2017). The "mgcv" package for GAM was used, developed by Wood and Wood (2015) in the R software (R 4.2.3, released on 2023/03/16) (R Core Team, 2023). The model was also checked by residual plots generated using the gam.check () function from the "mgcv" package.

2.7.2. ANOVA and HSD test

We conducted a One-way ANOVA and post-hoc analysis using Tukey's Honesty Significant Difference (HSD) test to identify significant differences in PM10 concentration, PM10 deposition flux, and PM10 dry deposition among the industrial, park, and roadside sampling sites. The Tukey HSD test was chosen for its effectiveness in controlling the likelihood of Type I errors and is appropriate in multiple comparisons across all possible group pairings (Agbangba et al., 2024; Toothaker, 1993). The significant difference in this context implies the mean differences among sites. The threshold for significance was a p-value of <0.05 ($p < 0.05$).

3. Results

3.1. The amount of green space percentage, the variation of PM10 concentration and PM10 deposition flux during the vegetation period

The amount of green space percentage, PM10 concentration, and PM10 deposition flux within a one-kilometre buffer surrounding the measuring stations varied across cities situated in different climate zones. The highest percentage of green space (36.5 %) was found in the sample sites in Melbourne, followed by Berlin (32.4 %). In contrast, the lowest percentage of green space (23 %) was found in the sample sites in Stockholm followed by Vancouver (23.2 %) (Supplementary Table 9).

The highest mean PM10 concentration (34 $\mu g/m^3$) and mean PM10 deposition flux (0.22 $\mu g/m^2/h$) were observed in Hong Kong, located in the humid subtropical climate zone (Cfa). Conversely, the lowest mean PM10 concentration (12 $\mu g/m^3$) and PM10 deposition flux (0.08 $\mu g/m^2/h$) were found in Vancouver, located in the oceanic climate (Cfb). Berlin showed the second-highest mean PM10 concentration (23.7 $\mu g/m^3$) and PM10 deposition flux (0.15 $\mu g/m^2/h$). Berlin was followed by Los Angeles which is located in the Mediterranean warm climate (Csa) (PM10 concentration of 21.9 $\mu g/m^3$ *and mean* PM10 deposition flux of 0.14 $\mu g/m^2/h$). The mean PM10 concentration and deposition flux in Stockholm (humid continental climate Dfb) were comparatively lower than those in Berlin, London, and Melbourne (Cfb). Melbourne had lower levels of PM10 concentration and PM10 deposition flux (0.13 $\mu g/m^2/h$) compared to London and Berlin, but higher than Vancouver.

However, PM10 concentration trends and distribution differed during the vegetation period, which consequently led to changes in the trends and distribution of PM10 deposition flux (Supplementary Table 8). Los Angeles ($P = 0.28$), Berlin, and Melbourne ($P < 0.001$) showed a decreasing trend of PM10 with an increasing trend of green space percentage (Fig. 4). In contrast, London, Stockholm, Vancouver, New York, and Hong Kong experienced a decline in PM10 concentration ($p < 0.001$), despite no concurrent increase in green space percentage. Notably, the green space percentage increased in one sample site in New York (NY110) and one in Hong Kong (HKTP) over the studied period.

3.2. Influence of climatic variables (precipitation, LST, and wind pressure) and population density on PM10 deposition flux

Both the Spearman correlation matrix and GAM model showed a significant impact of population density and climatic variables, namely precipitation, land surface temperature (LST), and wind pressure on PM10 deposition flux.

The Spearman correlation matrix showed a negative correlation ($r = -0.14$, $p < 0.05$) between PM10 deposition flux and precipitation. Besides this linear overview of the negative correlation in the correlation matrix, the GAM model also confirmed the negative correlation by showing a downward fitted curve in PM10 deposition flux with increasing precipitation beyond 750 mm. In contrast, PM10 deposition flux revealed a significant moderate positive relationship with both land surface temperature ($r = 0.42$, $p < 0.01$) and wind pressure ($r = 0.39$, $p < 0.01$) (Fig. 5). Similarly, the positive correlations between PM10 deposition flux, LST and wind pressure were also demonstrated by the GAM model, depicting upward fitted curve of both the LST and wind pressure above 17 °C and 8 kPa respectively (Fig. 6). PM10 deposition flux and population density revealed a weak positive ($r = 0.19$, $p < 0.01$) correlation indicating higher population density in studied cities is associated with higher PM10 concentration (Fig. 5). The GAM model also showed an upward trend in PM10 deposition flux with increasing population density (Fig. 6).

3.3. Impact of neighbourhood green space percentage on PM10 deposition flux and assessment of the model performance

The GAM model analysis showed a non-linear association between neighbourhood green space percentage and PM10 deposition flux (Effective Degrees of Freedom = 3.15, Reference Degrees of Freedom = 3.95, Chi-square = 19.53, p-value = 0.0006). However, the fitted curve in the GAM model exhibited a downward trend above 27 % of green space, where it fell below the horizontal line at zero. Initially, the fitted curve of PM10 deposition flux showed an upward trend and exceeded the horizontal line at zero when the green space percentage ranged between 10 and 20. Eventually, the fitted curve showed a downward trend above the 20 % green space level (Fig. 7).

The model explained the total deviance of the response variable of about 42.1 %. After adjusting for the number of predictor variables, the model explained 57 % of the variation in the response variable ($R^2 = 0.57$). The restricted maximum likelihood (REML) value of the model was −390.97. The goodness of model fit is better assessed through the AIC. The model with the lowest AIC value of −1485.3 was considered the best (Supplementary Table 15). The scale estimation of the model was 1. The assessed quantile-quantile (QQ) plot showed a slight deviation of the residuals from the normal distribution. The deviation of residuals was not statistically significant (Kolmogorov-Smirnov test: $P = 0.26 > 0.05$) (Fig. 7 B).

3.4. Comparison of emission sources – roadside vs industrial sites in relation to park sites as particulate matter sink

The PM10 concentration, PM10 deposition flux, and PM10 dry deposition differed significantly among industrial (Brent-Neasden), roadside (Islingdon-Holloway Road), and park (Camden-Bloomsbury)

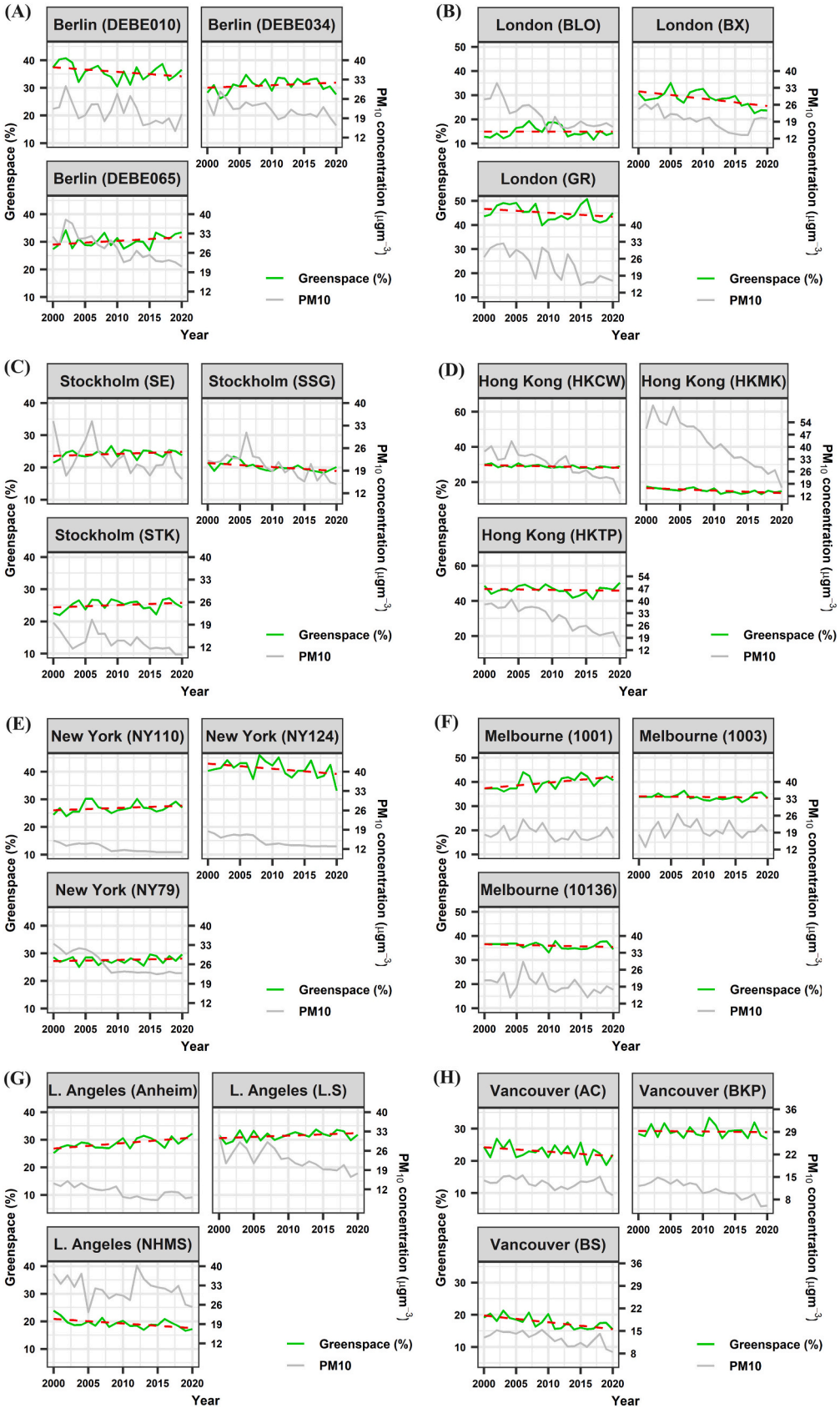

Fig. 4. The amount of greenspace percentage and variation of PM10 concentration over 20 years (2000–2020) within buffer area across sample sites; (A) for Berlin, (B) for London, (C) for Stockholm, (D) for Hong Kong, (E) for New York, (F) for Melbourne, (G) for Los-Angeles and (H) for Vancouver. The characters enclosed with parentheses in every figure indicate the sample site ID.

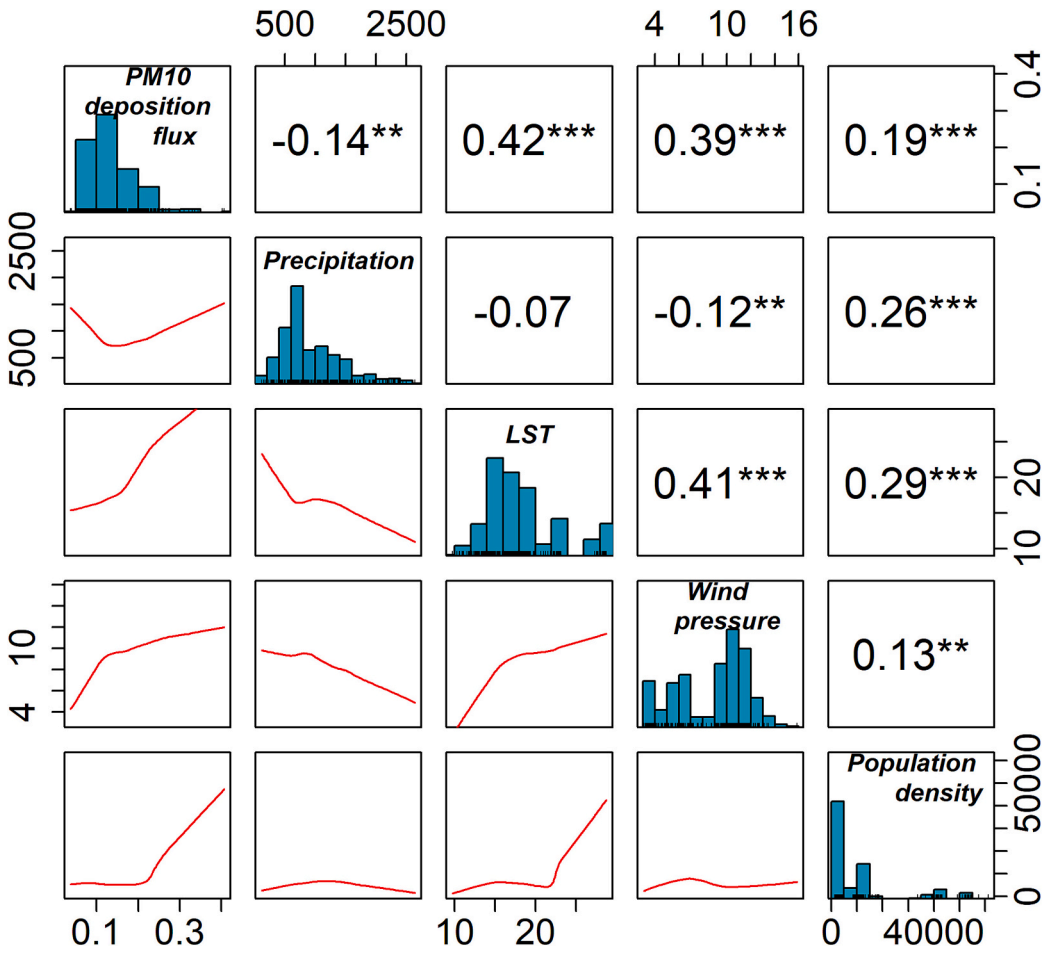

Fig. 5. The Spearman correlation coefficients among PM10 deposition flux, climatic variables, and population density.
The population density unit persons per square kilometre.
In the above plot: The distribution of each variable is shown on the diagonal.
On the bottom of the diagonal: the bivariate scatter plots with a fitted line are displayed.
On the top of the diagonal: the value of the correlation plus the significance level as stars.
Each significance level is associated with a symbol: *p*-values (0, 0.001, 0.01, 0.05, 0.1, 1).
<=> symbols ("***", "**", "*", ".", " ").

sample sites during the vegetation period (Supplementary Table 13).

The difference in PM10 concentration between the industrial and park sites was 20.54 μg/m^3 with P a value <0.001. The difference between the roadside and park sites was 5.41 μg/m^3, and the difference between industrial and roadside sites was 15.12 μg/m^3. Similarly, significant differences were also observed in PM10 deposition flux and dry deposition during the vegetation period. The highest difference was recorded between park and industrial sites (difference = 0.132 μg/m^2/*h*, and difference = 1974.9 μg/m^2/*day* respectively) (Fig. 8).

The highest mean PM10 concentration (40.89 μg/m^3) and PM10 deposition flux (0.26 μg/m^2/*h*) were observed in the industrial sampling site. Conversely, the park sample site (20.17 μg/m^3) had the lowest PM10 concentration and PM10 deposition flux (0.131 μg/m^2/*h*) (Fig. 8 A). Similarly, the largest mean amount of PM10 dry deposition (2723.87 μg/m^2/*day*) was measured at the industrial sample site, followed by the roadside (852.94 μg/m^2/*day*) (Fig. 8 C).

4. Discussion

4.1. The variation of PM10 concentration, PM10 deposition flux, and impacts of population density and climatic variables

Particulate matter is generally influenced by climatic variables, emissions, and chemical transformations (Seinfeld and Pandis, 2016). More than that, higher population density leads to higher sources of PM10 emissions (Baek and Ban 2020). As a result, the spatial distribution of PM shows high variability in space and is associated with the distribution of emission sources (Giorgi and Meleux, 2007). Consequently, PM10 concentration and deposition flux varied across our sample sites, despite all being within the same city. For instance, the sample sites of Hong Kong had the highest population density, located in a sub-tropical climate region characterized by hot and humid summers, and cool and dry winters. All sample sites in Hong Kong showed a decreasing trend of PM10 levels over the studied period, even though the amount of green space percentage did not show an increasing trend in the two sample sites. Similarly, the warm, hot summers of the sample sites in Los Angeles showed higher concentration and deposition flux compared to sample sites in London located in a warm temperate and Stockholm located in a humid continental climate, despite both cities having higher population density than Los Angeles.

Sample sites in Stockholm, with shorter, cooler summers and long, cold winters, likely have lower particulate matter concentrations and deposition than those in London and Berlin, despite Stockholm's higher population density. Although Berlin and London share similar Köppen climate classifications, London had lower average PM10 levels (21.73 μg/m^3) and deposition flux (0.14 μg/m^2/h) compared to Berlin. This

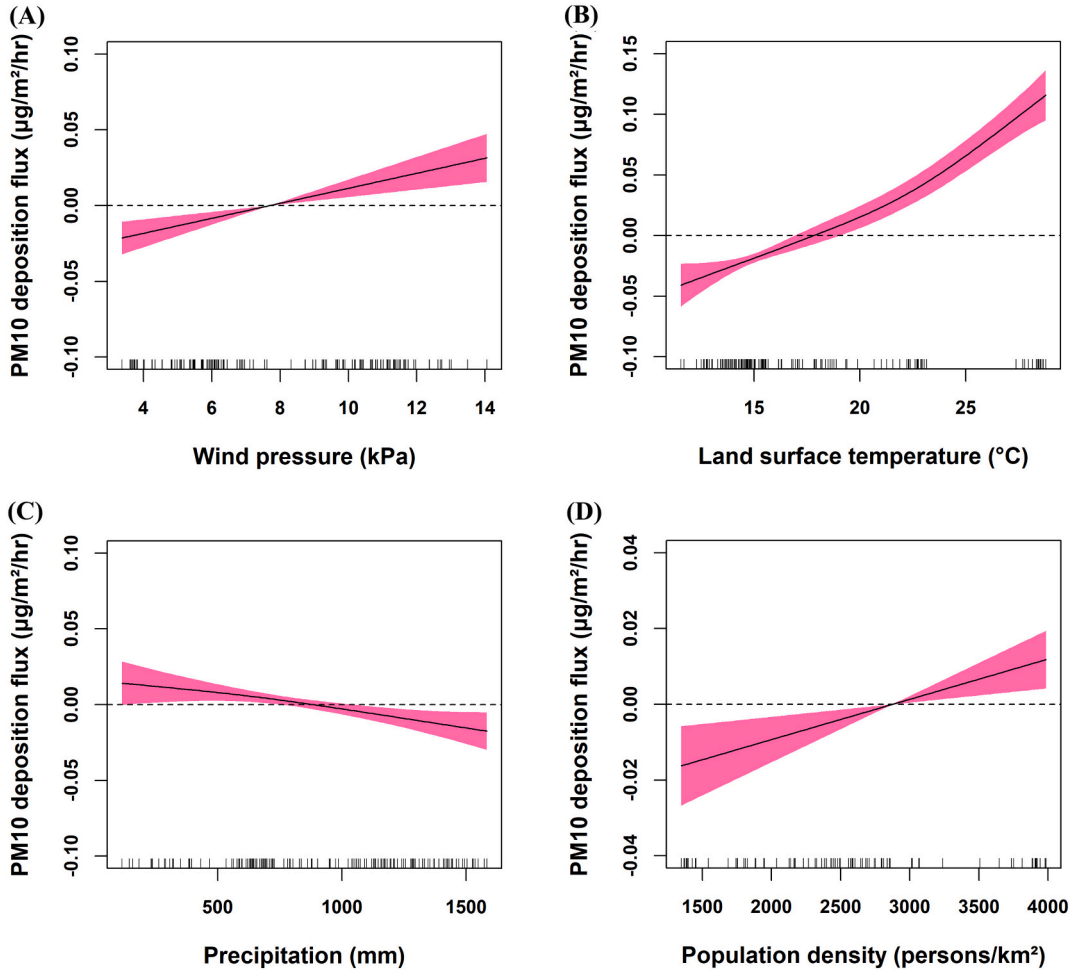

Fig. 6. (A), (B), (C), (D) are the partial effects of wind pressure, LST, precipitation, and population density respectively on PM10 deposition flux.

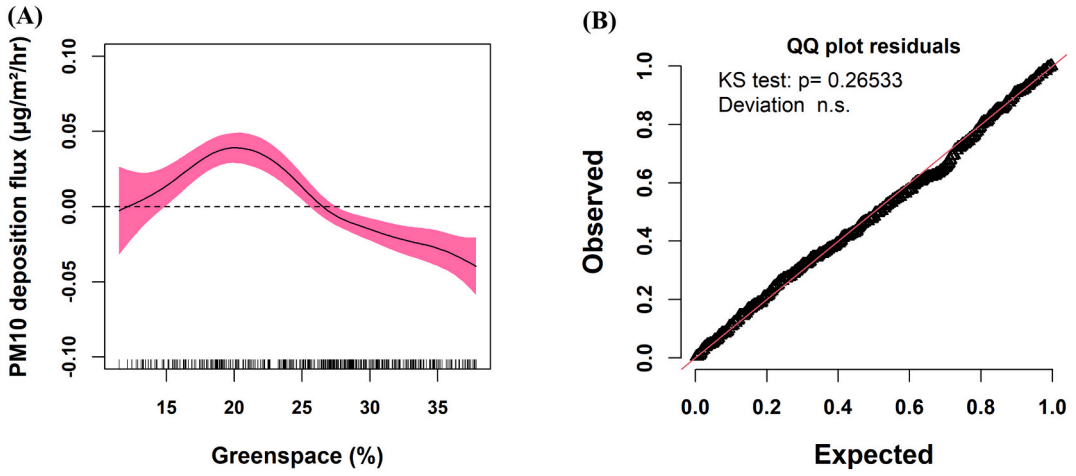

Fig. 7. (A) The partial effects of greenspace percentage on the PM10 deposition flux within a 1 km buffer area around air quality monitoring stations in sample sites. The tick marks on the x-axis are observed data points of the greenspace percentage and the x-axis indicated that no sample site with greenspace less than around 10 %. The y-axis represents the partial effect of greenspace percentage on PM10 deposition flux. The solid line represents the fitted curve of predictor variables. The shaded area indicated the 95 % confidence intervals. (B) Quantile - Quantile plot of observed residuals generated from GAM model (see supplementary Fig. 3 for GAM model check with residuals).

might also explain the general trend of decreasing particulate matter levels over all the sample sites, with the increase in awareness and countermeasures for reducing anthropogenic emissions. However, our findings are also in line with previous research such as Baró et al. (2015), who reported PM10 levels and dry deposition in Berlin (30.1 $\mu g/m^3$ and 19 kg/ha year) were higher than in Stockholm (28.5 $\mu g/m^3$ and 10.9 kg/ha year). Moreover, previous research showed that emissions vary across core metropolitan areas worldwide. For instance, Wei et al.

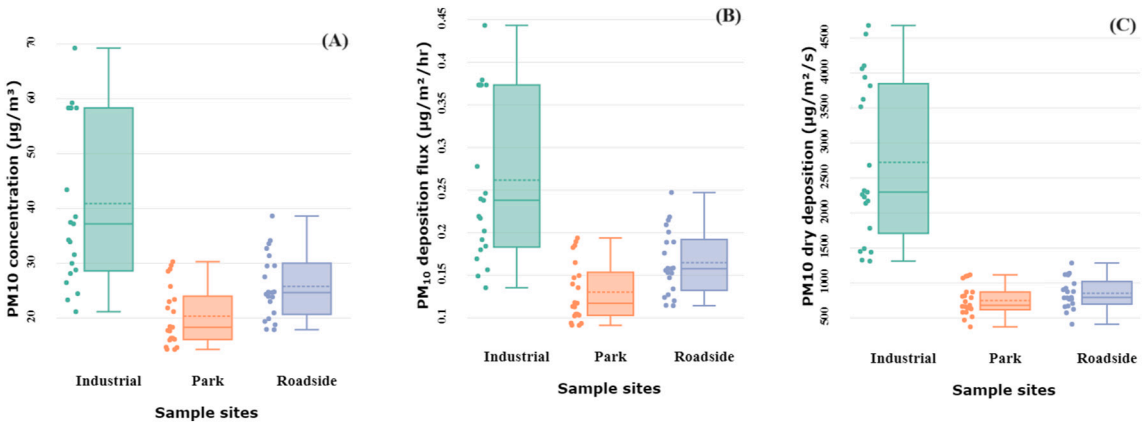

Fig. 8. (A). The mean PM10 concentration, (B) deposition flux, and (C) dry deposition in studied sample sites in London during the vegetation period from 2000 to 2020.

(2021) found that Stockholm had lower fuel combustion emissions (60 %) compared to North American cities (60–80 %) between 2009 and 2012. Los Angeles had higher transport emissions than Stockholm, Melbourne, and New York, but lower than Hong Kong. Our results are consistent with the city index proposed by the Greater London Authority (2014) regarding PM10 levels in different cities, showing Vancouver had the lowest PM10 levels among 36 cities, while Stockholm had lower PM10 than London, and Berlin had higher. Hong Kong had the highest PM10 levels among all studied cities.

More importantly, the present study showed that climatic variables e.g., precipitation, LST, and wind pressure along with population density have a significant impact on the PM10 deposition flux. Population density surrogates higher emissions that result in higher amounts of PM10. Consequently, we found a positive association between deposition flux and population density. Similarly, Dong et al. (2019) identified a significant positive relationship between population density and PM10 concentrations. The negative relationship or washout effect of precipitation and positive relations with wind pressure is consistent with the previous studies (Faisal et al., 2022; Li et al., 2019). In contrast to our findings, a negative effect of temperature was reported by Faisal et al. (2022) on the pollutant concentration during the winter season in Dhaka. Bangladesh is generally characterized by a humid and tropical climate, with distinct wet and dry seasons. The country typically experiences a monsoon season with heavy rainfall from June to October and a drier winter season from November to February. During the winter, the climate in Bangladesh is drier than during the monsoon season. Similarly, Li et al. (2019) reported negative correlations between temperature and pollutant concentration during spring and autumn over most of the regions of China. However, Li et al. (2019) reported positive relations during summer and winter. Our observed positive relationship between land surface temperature and PM10 deposition flux may be attributed to the assumption that higher temperatures can lead to soil drying, which leads to higher lifting of dust particles into the surroundings. Since surface moisture and surface temperature are inversely related (Tang and Chen, 2017). These findings have important implications, particularly with the advent of significant soil drought (Rahman et al., 2021), and increasing urban heat islands (Rahman et al., 2022; Rahman et al., 2023) in the near future. Therefore, a climate-sensitive urban greening or nature-based solution might have multi-dimensional benefits of reducing urban heating and PM concentration (Pauleit et al., 2011).

4.2. The impact of neighbourhood green space percentage on PM10 deposition flux

Our study revealed a non-linear association between neighbourhood green space percentage and PM10 deposition flux. There are inconsistent results in the literature regarding the role of urban green spaces in particulate matter removal. While studies like Qiu et al. (2018) and Manes et al. (2016) showed a significant impact of green spaces on air quality improvement, Venter et al. (2024) found only a minor decline (0.8 % over ten years) in urban air pollution and no significant effect at street level. Thus, our findings of increasing PM10 with <20 % green space warrant further investigation and might also hint at the fact that other land uses rather than green spaces contribute to higher particulate matter concentration. The scale of our study might also cause the anomalies as reported by Venter et al. (2024). Nevertheless, what is missing is the threshold that depicts the impact of green spaces. Our model suggests that at least 27 % of green spaces is needed to significantly reduce the particulate matter flux, although the minimum threshold can vary depending on the specific urban contexts.

After that, deposition flux starts decreasing below the zero fitted line to consistently increase the PM10 deposition rate (Fig. 7 A). However, it is important to note that we did not have quantitative measurements to determine the extent of the deposition flux reduction. Moreover, urban surface roughness contributes to higher PM concentration (Draxler et al., 2001). Further studies are needed for a detailed understanding of the extent of PM10 concentration and deposition flux and the role of green spaces in improving air quality. Furthermore, it should be kept in mind that the PM10 deposition velocity (V_d) is not solely dependent on the Leaf Area Index (LAI), but it is also influenced by site-specific temporal dynamics (Terzaghi et al., 2013). In our study, we used the same V_d value for all sample sites that could vary among sample sites.

However, based on these findings, it can be affirmed that urban vegetation plays an important role in reducing PM10 levels. Studies have shown that green space can cause PM to alter routes, speed, and other properties, or to be displaced from the air temporally or permanently (Diener and Mudu, 2021). Additionally, it is important to consider the climatic variables that affect the reduction of PM10 deposition flux to understand the magnitude of the impact of green space across different cities in contrasting climate zones. Thus, cities in warmer climate zones might require an additional amount of green spaces to combat the higher PM concentration since higher LST will increase the suspended particular matter concentration.

4.3. Strategic placement of urban green spaces: key to enhancing air quality

The PM10 concentration, deposition flux, and dry deposition were compared across different proximities to emission source types, e.g. industrial, roadside, and park in London. The emission from local transportation, particularly private and public vehicles, emits a large amount of particulate matter. As a follow-up, traffic is recognized as a common source of particulate matter (Sgrigna et al., 2015).

Consequently, the sample site in the roadside areas experienced higher levels of PM10 concentration and deposition flux compared to the sample site in the park. In the current study, the sample site in the industrial area was particularly exposed to coal and oil combustion in the industrial process along with the frequent presence of heavy vehicles which could exacerbate the emission (Wu et al., 2013). Those heavy vehicles and frequent stopping starting of vehicles might lead to higher emissions in congested areas. Our findings showed that the mean PM10 concentration (36.25 $\mu g/m^3$) was higher in industrial areas compared to roadside (25.73 $\mu g/m^3$) *and* park (20.17 $\mu g/m^3$). These findings are in line with previous research such as Millán-Martínez et al. (2021), who reported that industrial sites demonstrated higher contribution sources of PM10 concentration compared to road sites in Spain. Therefore, it is important to prioritize vegetation in areas with higher particulate matter concentration rather overall increase in the green cover to improve the air quality in cities. However, direct implementation of green covers such as dense tree rows might reduce the visibility of the traffic, therefore, strategic plantings such as shorter vegetation close to the curb and taller trees towards the center of the roadside islands might reduce the trade-offs.

4.4. Limitation

It needs to be kept in mind that deposition velocity (V_d) is site-specific and depends on canopy LAI, atmospheric conditions such as wind speed, relative humidity and air temperature and is also affected by site-specific temporal dynamics.

However, due to the scale of our study, we approximated the V_d value as a single value. Because we could not find any remotely sensed or monitoring data for site-specific V_d value for each city. Therefore, we do acknowledge it is a source of uncertainty in our analysis.

Additionally, although the findings provide valuable insights into the impact of the neighbourhood greenspace percentage, population density and climatic variable on PM10 deposition flux across diverse climate zones, the study did not include larger metropolises in tropical climates due to the unavailability of consistent PM10 concentrations data. Future research could be conducted solely in tropical climate zones changing the temporal period.

5. Conclusion

This study investigated the influence of neighbourhood green space density along with climatic variables and population density on PM10 deposition flux during the vegetation period over the twenty years (2000−2020) across studied cities located in different major climate zones. Cities with higher population density in warmer and drier climate zones tend to show higher PM concentrations since LST was positively correlated to the PM concentration and deposition flux. Therefore, highly populated cities in warmer climates might require a higher amount of green spaces as land cover to confer the PM10 levels in the future. Despite the decreasing trends of PM10 in all sample sites over the studied years, there was no concurrent increasing trend of green space percentages in a few sample sites. Therefore, reducing anthropogenic emissions by countermeasures and increasing awareness needs to also be considered and given priority. In the sample sites of London, the industrial site showed higher concentration and deposition flux values, including dry deposition. Thus, strategically placing urban green spaces (i.e., as close as possible to the emission source) is more important than merely increasing green cover.

Our study suggests the minimum threshold of 27 % of land cover with green spaces to have a significant effect on air quality by reducing PM10 flux, of course, the figure may vary depending on the specific urban contexts. In line with other climate change mitigation measures, for example, Rahman et al. (2022, 2024) prescribed at least 30–40 % green spaces to mitigate urban heat; our study is also in good alignment with the threshold for better air quality. Moreover, further investigation into including quantitative aspects of urban surface forms and transportation networks is still necessary.

CRediT authorship contribution statement

Azharul Islam: Writing – original draft, Visualization, Validation, Methodology, Investigation, Formal analysis, Data curation, Conceptualization. **Nayanesh Pattnaik:** Writing – review & editing, Formal analysis. **Md. Moktader Moula:** Data curation. **Thomas Rötzer:** Writing – review & editing, Resources. **Stephan Pauleit:** Writing – review & editing, Resources. **Mohammad A. Rahman:** Writing – review & editing, Resources, Methodology, Conceptualization.

Declaration of competing interest

All authors declare no conflict of financial interests or personal relationships that may be perceived as influencing their work.

Acknowledgements

Our gratitude to the following organizations: the Federal Environment Agency (Germany), Empirical College of London (Great Britain), Swedish Meteorological and Hydrological Institute (Sweden), Environment Protection Authority, Victoria (Australia), Environmental Protection Department (Hong Kong, China), Government of British Columbia (Canada), Environmental Protection Agency (USA), who made PM data publicly available for research groups. We adhere to the data usage license and respect the terms and conditions outlined in the license in using PM data for this study. The graphical abstract was created with BioRender.com (NM25XL4P0G) with a purchased license. Thanks also go to the German Research Foundation (Deutsche Forschungsgemeinschaft) for providing funds for the projects 437788427 - RTG 2679, and PR 292/21-1 and PA 2626/3-1 'Impact of trees on the urban microclimate under climate change: mechanisms and ecosystem services of urban tree species in temperate, Mediterranean and arid major cities'.

Appendix A. Supplementary data

Supplementary data to this article can be found online at https://doi.org/10.1016/j.scitotenv.2024.176770.

Data availability

Data will be made available on request.

References

Agbangba, Codjo Emile, Aide, Edmond Sacla, Honfo, Hermann, Kakai, Romain Glèlè, 2024. On the use of post-hoc tests in environmental and biological sciences: a critical review. Heliyon 10 (3), e25131. https://doi.org/10.1016/j.heliyon.2024.e25131.

Akyüz, Mehmet, Çabuk, Hasan, 2009. Meteorological variations of PM2.5/PM10 concentrations and particle-associated polycyclic aromatic hydrocarbons in the atmospheric environment of Zonguldak, Turkey. J. Hazard. Mater. 170 (1), 13–21. https://doi.org/10.1016/j.jhazmat.2009.05.029.

An, Xingqin, Hou, Qing, Li, Nan, Zhai, Shixian, 2013. Assessment of human exposure level to PM10 in China. Atmos. Environ. 70, 376–386. https://doi.org/10.1016/j.atmosenv.2013.01.017.

Andalibi, Lida, Ghorbani, Ardavan, Moameri, Mehdi, Hazbavi, Zeinab, Nothdurft, Arne, Jafari, Reza, Dadjou, Farid, 2021. Leaf area index variations in ecoregions of Ardabil Province, Iran. J. Remote Sens. 13 (15), 2879. https://doi.org/10.3390/rs13152879.

Anderson, Jonathan O., Thundiyil, Josef G., Stolbach, Andrew, 2012. Clearing the air: a review of the effects of particulate matter air pollution on human health. J. Med. Toxicol. 8 (2), 166–175. https://doi.org/10.1007/s13181-011-0203-1.

Arshad, Hafiz Syed Hamid, Kumar Routray, Jayant, 2018. From socioeconomic disparity to environmental injustice: the relationship between housing unit density and community green space in a Medium City in Pakistan. Local Environ. 23 (5), 536–548. https://doi.org/10.1080/13549839.2018.1442424.

Augustin, Nicole, Sauleau, Eric-Andre, Wood, Simon, 2012. On quantile quantile plots for generalized linear models. Comput. Stat. Data Anal. 56 (8), 2404–2409. https://doi.org/10.1016/j.csda.2012.01.026.

Baró, Francesc, Haase, Dagmar, Gómez-Baggethun, Erik, Frantzeskaki, Niki, 2015. Mismatches between ecosystem services supply and demand in urban areas: a quantitative assessment in five European cities. Ecol. Indic. 55, 146–158. https://doi.org/10.1016/j.ecolind.2015.03.013.

Burnham, Kenneth P., Anderson, David R., 2004. Multimodel inference: understanding AIC and BIC in model selection. Sociol. Methods Res. 33 (2), 261–304. https://doi.org/10.1177/0049124104268644.

Chithra, V.S., Shiva Nagendra, S.M., 2014. Impact of outdoor meteorology on indoor PM10, PM2.5 and PM1 concentrations in a naturally ventilated classroom. Urban Clim. 10, 77–91. https://doi.org/10.1016/j.uclim.2014.10.001.

Chowdhury, Pratiti Home, Okano, Hitoshi, Honda, Akiko, Kudou, Hitomi, Kitamura, Gaku, Ito, Sho, Ueda, Kayo, Takano, Hirohisa, 2018. Aqueous and organic extract of PM2.5 collected in different seasons and cities of Japan differently affect respiratory and immune systems. Environ. Pollut. 235, 223–234. https://doi.org/10.1016/j.envpol.2017.12.040.

Connors, John Patrick, Galletti, Christopher S., Chow, Winston T.L., 2013. Landscape configuration and urban Heat Island effects: assessing the relationship between landscape characteristics and land surface temperature in Phoenix, Arizona. Landsc. Ecol. 28 (2), 271–283. https://doi.org/10.1007/s10980-012-9833-1.

Cowell, Whitney J., Brunst, Kelly J., Malin, Ashley J., Coull, Brent A., Gennings, Chris, Kloog, Itai, Lipton, Lianna, Wright, Robert O., Enlow, Michelle Bosquet, Wright, Rosalind J., 2019. Prenatal exposure to PM2.5 and cardiac vagal tone during infancy: findings from a multiethnic birth cohort. Environ. Health Perspect. 127 (10), 107007. https://doi.org/10.1289/EHP4434.

De Peppo, Margherita, Taramelli, Andrea, Boschetti, Mirco, Mantino, Alberto, Volpi, Iride, Filipponi, Federico, Tornato, Antonella, Valentini, Emiliana, Ragaglini, Giorgio, 2021. Non-parametric statistical approaches for leaf area index estimation from Sentinel-2 data: a multi-crop assessment. Remote Sens. 13 (14), 2841.

Deshmukh, Parikshit, Isakov, Vlad, Venkatram, Akula, Bo Yang, K., Zhang, Max, Logan, Russell, Baldauf, Richard, 2019. The effects of roadside vegetation characteristics on local, near-road air quality. Air Qual. Atmos. 12 (3), 259–270. https://doi.org/10.1007/s11869-018-0651-8.

Diener, Arnt, Mudu, Pierpaolo, 2021. How can vegetation protect us from air pollution? A critical review on green Spaces' mitigation abilities for air-borne particles from a public health perspective - with implications for urban planning. Sci. Total Environ. 796, 148605. https://doi.org/10.1016/j.scitotenv.2021.148605.

Dong, Kangyin, Hochman, Gal, Kong, Xianli, Sun, Renjin, Wang, Zhiyuan, 2019. Spatial econometric analysis of China's PM10 pollution and its influential factors: evidence from the provincial level. Ecol. Indic. 96, 317–328. https://doi.org/10.1016/j.ecolind.2018.09.014.

Draxler, Roland R., Gillette, Dale A., Kirkpatrick, Jeffrey S., Heller, Jack, 2001. Estimating PM10 air concentrations from dust storms in Iraq, Kuwait and Saudi Arabia. Atmos. Environ. 35 (25), 4315–4330. https://doi.org/10.1016/S1352-2310(01)00159-5.

Erisman, Jan Willem, Draaijers, Geert, 2003. Deposition to forests in Europe: Most important factors influencing dry deposition and models used for generalisation. Environ. Pollut. 124 (3), 379–388. https://doi.org/10.1016/S0269-7491(03)00049-6.

Faisal, Abdullah-Al, Abdulla-Al Kafy, Md., Fattah, Abdul, Dewan, Md., Jahir, Amir, Al Rakib, Abdullah, Rahaman, Zullyadini A., Ferdousi, Jannatul, Huang, Xiao, 2022. Assessment of temporal shifting of PM2.5, lockdown effect, and influences of seasonal meteorological factors over the fastest-growing megacity, Dhaka. Spat. Inf. Res. 30 (3), 441–453. https://doi.org/10.1007/s41324-022-00441-w.

Gao, Guojun, Sun, Fengbin, Thao, Nguyen Thi Thanh, Lun, Xiaoxiu, Xinxiao, Yu., 2015. Different concentrations of TSP, PM 10, PM 2.5, and PM 1 of several urban forest types in different seasons. Pol. J. Environ. Stud. 24 (6), 2387–2395. https://doi.org/10.15244/pjoes/59501.

Giorgi, Filippo, Meleux, Frédérick, 2007. Modelling the regional effects of climate change on air quality. Compt. Rendus Geosci. 339 (11), 721–733. https://doi.org/10.1016/j.crte.2007.08.006.

González-Andrés, Cristina, Sánchez-Lizaso, José Luís, Cortés, Jorge, Pennino, Maria Grazia, 2021. Predictive habitat suitability models to aid the conservation of elasmobranchs in Isla Del coco National Park (Costa Rica). J. Mar. Syst. 224, 103643. https://doi.org/10.1016/j.jmarsys.2021.103643.

Greater London Authority: London, UK, 2014. Comparison of air quality in london with a number of world and European cities. Retrieved from. https://www.london.gov.uk/sites/default/files/comparison_of_air_quality_in_world_cities_study_final.pdf.

Gromke, Christof, Ruck, Bodo, 2009. On the impact of trees on dispersion processes of traffic emissions in street canyons. Boundary-Layer Meteorol. 131 (1), 19–34. https://doi.org/10.1007/s10546-008-9301-2.

Gunawardena, Kanchane R., Wells, Martin J., Kershaw, Tristan, 2017. Utilising green and Bluespace to mitigate urban Heat Island intensity. Sci. Total Environ. 584, 1040–1055.

Hartig, Florian, Hartig, Maintainer Florian, 2017. Package 'DHARMa.'. R Package.

Henry, Christophe, Minier, Jean-Pierre, Brambilla, Sara, 2023. Particle resuspension: challenges and perspectives for future models. Phys. Rep. 1007, 1–98. https://doi.org/10.1016/j.physrep.2022.12.005.

Huete, A.R., Liu, H.Q., Batchily, K., van Leeuwen, W., 1997. A comparison of vegetation indices over a global set of TM images for EOS-MODIS. Remote Sens. Environ. 59 (3), 440–451. https://doi.org/10.1016/S0034-4257(96)00112-5.

Baek, Jong In, Ban, Yong Un, 2020. The impacts of urban air pollution emission density on air pollutant concentration based on a panel model. Sustainability 12 (20), 8401. https://doi.org/10.3390/su12208401.

Janhäll, Sara, 2015. Review on urban vegetation and particle air pollution–deposition and dispersion. Atmos. Environ. 105, 130–137. https://doi.org/10.1016/j.atmosenv.2015.01.052.

Kang, Hyun, 2013. The prevention and handling of the missing data. Korean J. Anesthesiol. 64 (5), 402–406. https://doi.org/10.4097/kjae.2013.64.5.402.

Langner, Marcel, Kull, Martin, Endlicher, Wilfried R., 2011. Determination of PM10 deposition based on antimony flux to selected urban surfaces. Environ. Pollut. 159 (8), 2028–2034. https://doi.org/10.1016/j.envpol.2011.01.017.

Lei, Yakai, Duan, Yanbo, He, Dan, Zhang, Xiwen, Chen, Lanqi, Yonghua Li, Yu, Gao, Gary, Tian, Guohang, Zheng, Jingbiao, 2018. Effects of urban greenspace patterns on particulate matter pollution in metropolitan Zhengzhou in Henan, China. Atmosphere 9 (5), 199. https://doi.org/10.3390/atmos9050199.

Li, Xiaoyang, Song, Hongquan, Zhai, Shiyan, Siqi, Lu, Kong, Yunfeng, Xia, Haoming, Zhao, Haipeng, 2019. Particulate matter pollution in Chinese cities: areal-temporal variations and their relationships with meteorological conditions (2015–2017). Environ. Pollut. 246, 11–18. https://doi.org/10.1016/j.envpol.2018.11.103.

London Air Quality Network, 2023. Welcome to the London Air Quality Network "Statistics Maps." Retrieved July 25. https://www.londonair.org.uk/london/asp/classification.asp?region=0&site=KC1&details=general&mapview=all&la_id=&network=All&MapType=Google.

Lovett, Gary M., 1994. Atmospheric deposition of nutrients and pollutants in North America: An ecological perspective. Ecol. Appl. 4 (4), 630–650. https://doi.org/10.2307/1941997.

Manes, F., Marando, F., Capotorti, G., Blasi, C., Salvatori, E., Fusaro, L., Ciancarella, L., Mircea, M., Marchetti, M., Chirici, G., Munafò, M., 2016. Regulating ecosystem Services of Forests in ten Italian metropolitan cities: air quality improvement by PM10 and O3 removal. Ecol. Indic. 67, 425–440. https://doi.org/10.1016/j.ecolind.2016.03.009.

Marando, Federica, Salvatori, Elisabetta, Fusaro, Lina, Manes, Fausto, 2016. Removal of PM10 by forests as a nature-based solution for air quality improvement in the Metropolitan City of Rome. Forests 7 (7), 150.

McDonald, A.G., Bealey, W.J., Fowler, D., Dragosits, U., Skiba, U., Smith, R.I., Donovan, R.G., Brett, H.E., Hewitt, C.N., Nemitz, E., 2007. Quantifying the effect of urban tree planting on concentrations and depositions of PM10 in two UK conurbations. Atmos. Environ. 41 (38), 8455–8467. https://doi.org/10.1016/j.atmosenv.2007.07.025.

McPherson, Gregory E., Nowak, David J., Rowntree, Rowan A., 1994. "Chicago's Urban Forest Ecosystem: Results of the Chicago Urban Forest Climate Project." Gen. Tech. Rep. NE-186. Radnor, PA: U. S. Department of Agriculture, Forest Service, Northeastern Forest Experiment Station. 201 p. 186. https://doi.org/10.2737/NE-GTR-186.

Millán-Martínez, María, Daniel Sánchez-Rodas, A.M., de la Campa, Sánchez, Alastuey, Andrés, Querol, Xavier, de la Rosa, Jesús D., 2021. Source contribution and origin of PM10 and arsenic in a complex industrial region (Huelva, SW Spain). Environ. Pollut. 274, 116268. https://doi.org/10.1016/j.envpol.2020.116268.

Moritz, Steffen, Bartz-Beielstein, Thomas, 2017. imputeTS: time series missing value imputation in R. R Journal 9 (1).

Nguyen, Quang-Viet, Liou, Yuei-An, 2024. Greenspace pattern, meteorology and air pollutant in Taiwan: a multifaceted connection. Sci. Total Environ. 914, 169883. https://doi.org/10.1016/j.scitotenv.2024.169883.

O'brien, Robert M., 2007. A caution regarding rules of thumb for variance inflation factors. Qual. Quant. 41 (5), 673–690. https://doi.org/10.1007/s11135-006-9018-6.

Ottosen, Thor-Bjørn, Kumar, Prashant, 2020. The influence of the vegetation cycle on the mitigation of air pollution by a deciduous roadside hedge. Sustain. Cities Soc. 53, 101919. https://doi.org/10.1016/j.scs.2019.101919.

Pace, Rocco, De Fino, Francesco, Rahman, Mohammad A., Pauleit, Stephan, Nowak, David J., Grote, Rüdiger, 2021. A single tree model to consistently simulate cooling, shading, and pollution uptake of urban trees. Int. J. Biometeorol. 65 (2), 277–289. https://doi.org/10.1007/s00484-020-02030-8.

Pauleit, Stephan, Liu, Li, Ahern, Jack, Kazmierczak, Aleksandra, 2011. "Multifunctional Green Infrastructure Planning to Promote Ecological Services in the City." P. 0 in Urban Ecology: Patterns, Processes, and Applications, edited by J. Niemelä, J. H. Breuste, T. Elmqvist, G. Guntenspergen, P. James, and N. E. McIntyre. Oxford University Press.

Peel, M.C., Finlayson, B.L., McMahon, T.A., 2007. Updated world map of the Köppen-Geiger climate classification. Hydrol. Earth Syst. Sci. 11 (5), 1633–1644. https://doi.org/10.5194/hess-11-1633-2007.

Pražnikar, Jure, 2017. Particulate matter time-series and Köppen-Geiger climate classes in North America and Europe. Atmos. Environ. 150, 136–145.

Qiu, Ling, Liu, Fang, Zhang, Xiang, Gao, Tian, 2018. The reducing effect of green spaces with different vegetation structure on atmospheric particulate matter concentration in BaoJi City, China. Atmosphere 9 (9), 332. https://doi.org/10.3390/atmos9090332.

R Core Team, 2023. R Core Team R: A Language and Environment for Statistical Computing. Foundation for Statistical Computing.

Rafael, S., Vicente, B., Rodrigues, V., Miranda, A.I., Borrego, C., Lopes, M., 2018. Impacts of green infrastructures on aerodynamic flow and air quality in Porto's urban area. Atmos. Environ. 190, 317–330. https://doi.org/10.1016/j.atmosenv.2018.07.044.

Rahman, Mohammad A., Dervishi, Vjosa, Moser-Reischl, Astrid, Ludwig, Ferdinand, Pretzsch, Hans, Rötzer, Thomas, Pauleit, Stephan, 2021. Comparative analysis of shade and underlying surfaces on cooling effect. Urban For. Urban Green. 63, 127223. https://doi.org/10.1016/j.ufug.2021.127223.

Rahman, Mohammad A., Franceschi, Eleonora, Pattnaik, Nayanesh, Moser-Reischl, Astrid, Hartmann, Christian, Paeth, Heiko, Pretzsch, Hans, Rötzer, Thomas, Pauleit, Stephan, 2022. Spatial and temporal changes of outdoor thermal stress:

influence of urban land cover types. Sci. Rep. 12 (1), 671. https://doi.org/10.1038/s41598-021-04669-8.
Rahman, Mohammad A., Pawijit, Yanin, Chao, Xu, Moser-Reischl, Astrid, Pretzsch, Hans, Rötzer, Thomas, Pauleit, Stephan, 2023. A comparative analysis of urban forests for storm-water management. Sci. Rep. 13 (1), 1451. https://doi.org/10.1038/s41598-023-28629-6.
Rahman, Mohammad A., Arndt, Stefan, Bravo, Felipe, Cheung, Pui K., van Doorn, Natalie, Franceschi, Eleonora, del Río, Miren, Livesley, Stephen J., Moser-Reischl, Astrid, Pattnaik, Nayanesh, Rötzer, Thomas, Paeth, Heiko, Pauleit, Stephan, Preisler, Yakir, Pretzsch, Hans, Tan, Puay Yok, Cohen, Shabtai, Szota, Chris, Torquato, Patricia R., 2024. More than a canopy cover metric: influence of canopy quality, water-use strategies and site climate on urban Forest cooling potential. Landsc. Urban Plan. 248, 105089. https://doi.org/10.1016/j.landurbplan.2024.105089.
Rötzer, Thomas, Frank-M. Chmielewski., 2001. Phenological maps of Europe. Inter-Res. Sci. Publ. 18 (3), 249–257. https://doi.org/10.3354/cr018249.
Seinfeld, John H., Pandis, Spyros N., 2016. Atmospheric Chemistry and Physics: From Air Pollution to Climate Change, 3rd Edition | Wiley. 3rd ed. Wiley.
Sgrigna, G., Sæbø, A., Gawronski, S., Popek, R., Calfapietra, C., 2015. Particulate matter deposition on Quercus Ilex leaves in an Industrial City of Central Italy. Environ. Pollut. 197, 187–194. https://doi.org/10.1016/j.envpol.2014.11.030.
Sohrab, Seyedehmehrmanzar, Csikós, Nándor, Szilassi, Péter, 2022. Connection between the spatial characteristics of the road and railway networks and the air pollution (PM10) in urban–rural fringe zones. Sustainability 14 (16), 10103. https://doi.org/10.3390/su141610103.
Sohrab, Seyedehmehrmanzar, Csikos, Nándor, Szilassi, Péter, 2023. Effects of land use patterns on PM10 concentrations in urban and suburban areas. A European scale analysis. Atmos. Pollut. Res. 14 (12), 101942. https://doi.org/10.1016/j.apr.2023.101942.
Tang, Chunling, Chen, Dong, 2017. Interaction between soil moisture and air temperature in the Mississippi River Basin. J. Water Resour. Protect. 9 (10), 1119.
Terzaghi, Elisa, Wild, Edward, Zacchello, Gabriele, Cerabolini, Bruno E.L., Jones, Kevin C., Di Guardo, Antonio, 2013. Forest filter effect: role of leaves in capturing/releasing air particulate matter and its associated PAHs. Atmos. Environ. 74, 378–384. https://doi.org/10.1016/j.atmosenv.2013.04.013.
Toothaker, Larry, 1993. Multiple Comparison Procedures. 2455 Teller Road, Thousand Oaks California 91320 United States of. SAGE Publications, Inc, America.
United Nations, 2018. Revision of World Urbanization Prospects. United Nations. Retrieved July 25, 2023. https://www.un.org/en/desa/2018-revision-world-urbanization-prospects.
Vashist, Mallika, Kumar, Thangamani Vijaya, Singh, Santosh Kumar, 2024. A comprehensive review of urban vegetation as a nature-based solution for sustainable Management of Particulate Matter in ambient air. Environ. Sci. Pol. 31 (18), 26480–26496. https://doi.org/10.1007/s11356-024-33089-0.
Venter, Zander S., Hassani, Amirhossein, Stange, Erik, Schneider, Philipp, Castell, Núria, 2024. Reassessing the role of urban green space in air pollution control. Proc. Natl. Acad. Sci. USA 121 (6), e2306200121. https://doi.org/10.1073/pnas.2306200121.
Vitaliano, Serena, Cascone, Stefano, D'Urso, Provvidenza Rita, 2024. Mitigating built environment air pollution by green systems: An in-depth review. Appl. Sci. 14 (15), 6487. https://doi.org/10.3390/app14156487.
Wang, Honglei, Tan, Yue, Zhang, Lianxia, Shen, Lijuan, Zhao, Tianliang, Dai, Qihang, Guan, Tianyi, Ke, Yue, Li, Xia, 2021. Characteristics of air quality in different climatic zones of China during the COVID-19 lockdown. Atmos. Pollut. Res. 12 (12), 101247.
Wang, Huixia, Shi, Hui, Li, Yangyang, Ya, Yu, Zhang, Jun, 2013. Seasonal variations in leaf capturing of particulate matter, surface wettability and micromorphology in urban tree species. Front. Environ. Sci. Eng. 7 (4), 579–588. https://doi.org/10.1007/s11783-013-0524-1.
Wang, Huixia, Shi, Hui, Wang, Yanhui, 2015. Effects of weather, time, and pollution level on the amount of particulate matter deposited on leaves of Ligustrum Lucidum. Sci. World J. 2015, 935942. https://doi.org/10.1155/2015/935942.
Wang, Xiaoshuang, Zhou, Zhixiang, Xiang, Yang, Peng, Chucai, Peng, Changhui, 2024. Effects of street plants on atmospheric particulate dispersion in urban streets: a review. Environ. Rev. 32 (1), 114–130. https://doi.org/10.1139/er-2023-0103.
Wei, Ting, Junliang, Wu, Chen, Shaoqing, 2021. Keeping track of greenhouse gas emission reduction Progress and targets in 167 cities worldwide. Front. Sustain. Cities 3.
Wood, Simon N., Augustin, Nicole H., 2002. GAMs with integrated model selection using penalized regression splines and applications to environmental modelling. Ecol. Model. 157 (2), 157–177. https://doi.org/10.1016/S0304-3800(02)00193-X.
Wood, Simon, Wood, Maintainer Simon, 2015. Package 'Mgcv.'. R Package Version 1 (29), 729.
Wu, Gang, Xin, Du, Xuefang, Wu, Xiao, Fu, Kong, Shaofei, Chen, Jianhua, Wang, Zongshuang, Bai, Zhipeng, 2013. Chemical composition, mass closure and sources of atmospheric PM10 from industrial sites in Shenzhen, China. J. Environ. Sci. 25 (8), 1626–1635. https://doi.org/10.1016/S1001-0742(12)60238-1.
Wu, Xianhua, Guo, Ji, 2021. Spatial concentration, impact factors and prevention-control measures of PM2.5 pollution in China. In: Economic Impacts and Emergency Management of Disasters in China. Springer Nature Singapore, Singapore, pp. 479–506.
Wu, Yanan, Liu, Jiakai, Zhai, Jiexiu, Ling Cong, Yu, Wang, Wenmei Ma, Zhang, Zhenming, Li, Chunyi, 2018. Comparison of dry and wet deposition of particulate matter in near-surface waters during summer. PLoS One 13 (6), e0199241. https://doi.org/10.1371/journal.pone.0199241.
Xu, Xiaowu, Zhang, Zhenming, Bao, Le, Mo, Li, Xinxiao, Yu, Fan, Dengxing, Lun, Xiaoxiu, 2017. Influence of rainfall duration and intensity on particulate matter removal from plant leaves. Sci. Total Environ. 609, 11–16. https://doi.org/10.1016/j.scitotenv.2017.07.141.
Yee, Thomas W., Mitchell, Neil D., 1991. Generalized additive models in plant ecology. J. Veg. Sci. 2 (5), 587–602. https://doi.org/10.2307/3236170.
Zellner, R., 1986. Papers of the Workshop Held at Frankfurt am Main, 5 to 6 February 1986 (Dechema Monographien). Wiley-VCH Verlag GmbH.
Zhang, Biao, Xie, Gao-di, Li, Na, Wang, Shuo, 2015. Effect of urban green space changes on the role of rainwater runoff reduction in Beijing, China. Landsc. Urban Plan. 140, 8–16. https://doi.org/10.1016/j.landurbplan.2015.03.014.
Zhao, Songting, Li, Xinyu, Li, Yanming, Li, Jiale, Liu, Xiuping, Duan, Minjie, Wang, Xing, 2024. Differential impacts of functional traits across 65 plant species on PM retention in the urban environment. Ecol. Eng. 200, 107184. https://doi.org/10.1016/j.ecoleng.2024.107184.
Zinke, Paul J., 1967. Forest Interception Studies in the United States. Pergamon Press Oxford, Oxford, UK.
Zufall, M.J., Davidson, C.I., 1998. "Dry Deposition of Particles from the Atmosphere." Pp. 55–73 in Air Pollution in the Ural Mountains: Environmental, Health and Policy Aspects. Vol. 40, NATO ASI Series, edited by I. Linkov and R. Wilson. Dordrecht: Springer Netherlands.
Zuur, Alain F., Ieno, Elena N., Smith, Graham M., 2007. Analysing Ecological Data. Springer New York, New York, NY.